TECHNICAL REPORT BRL-TR-3333

BRL

TOMOGRAPHIC RECONSTRUCTION OF INFRARED SPECTRA OF NONHOMOGENEOUS MEDIA: APPLICATIONS TO A FLAT FLAME BURNER

KEVIN L. McNESBY
ROBERT A. FIFER

APRIL 1992

U.S. ARMY LABORATORY COMMAND

BALLISTIC RESEARCH LABORATORY
ABERDEEN PROVING GROUND, MARYLAND

NOTICES

Destroy this report when it is no longer needed. DO NOT return it to the originator.

Additional copies of this report may be obtained from the National Technical Information Service, U.S. Department of Commerce, 5285 Port Royal Road, Springfield, VA 22161.

The findings of this report are not to be construed as an official Department of the Army position, unless so designated by other authorized documents.

The use of trade names or manufacturers' names in this report does not constitute indorsement of any commercial product.

REPORT DOCUMENTATION PAGE

Form Approved
OMB No. 0704-0188

1. AGENCY USE ONLY (Leave blank)	2. REPORT DATE	3. REPORT TYPE AND DATES COVERED
	April 1992	Final, Sep - Dec 91

4. TITLE AND SUBTITLE

Tomographic Reconstruction of Infrared Spectra of Nonhomogeneous Media: Applications to a Flat Flame Burner

5. FUNDING NUMBERS

PR: 1L161102AH43

6. AUTHOR(S)

Kevin L. McNesby and Robert A. Fifer

7. PERFORMING ORGANIZATION NAME(S) AND ADDRESS(ES)

8. PERFORMING ORGANIZATION REPORT NUMBER

BRL-TR-3333

9. SPONSORING / MONITORING AGENCY NAME(S) AND ADDRESS(ES)

U.S. Army Ballistic Research Laboratory
ATTN: SLCBR-DD-T
Aberdeen Proving Ground, MD 21005-5066

10. SPONSORING / MONITORING AGENCY REPORT NUMBER

11. SUPPLEMENTARY NOTES

12a. DISTRIBUTION / AVAILABILITY STATEMENT

Approved for public release; distribution is unlimited.

12b. DISTRIBUTION CODE

13. ABSTRACT *(Maximum 200 words)*

We are using computed tomography, a radiological imaging technique, to obtain species profiles within a flame as a function of height above the burner surface and lateral position at that height. This information is extracted from parallel line-of-sight absorbance data using a technique known as Abel inversion. This process yields two dimensional "slices" of the flame. At any point within each slice the infrared spectrum of the species present may be obtained. Abel inversion is a special application of computerized tomography which may be applied only to systems possessing axial symmetry.

We have used this technique to evaluate line-of-sight infrared spectra of a low pressure (< 100 torr) premixed methane/nitrous oxide burner flame. The flame is supported on a water-cooled, stainless steel cylindrical frit which sits inside a low pressure chamber. Parallel line-of-sight infrared spectra through the low pressure chamber are inverted to give the radial dependence of infrared absorption at each wavelength of the spectrum. This data is used to evaluate the performance of the low pressure burner and to discriminate against "cold" gases which may obscure absorbances of trace species within the flame.

14. SUBJECT TERMS	15. NUMBER OF PAGES
experimental methods, laminar flames, infrared spectroscopy, tomography	37
	16. PRICE CODE

17. SECURITY CLASSIFICATION OF REPORT	18. SECURITY CLASSIFICATION OF THIS PAGE	19. SECURITY CLASSIFICATION OF ABSTRACT	20. LIMITATION OF ABSTRACT
UNCLASSIFIED	UNCLASSIFIED	UNCLASSIFIED	UL

INTENTIONALLY LEFT BLANK.

TABLE OF CONTENTS

INTENTIONALLY LEFT BLANK.

LIST OF FIGURES

INTENTIONALLY LEFT BLANK.

1. INTRODUCTION

The study of low pressure flames has significance to the Army because these flames may provide information regarding the initial decomposition mechanisms of nitramine-based propellants (Schoeder 1980). In general, the flames under study are mixtures of a nitrogen-containing oxidizer and a conventional fuel. In the work reported here, a stoichiometric methane/nitrous oxide gas mixture is used because of the ease of working with this flame.

In a low pressure environment, the structure of a flame is expanded. Flame regions which hold the most interest for chemists and physicists are those in which chemical bonds are being broken and formed. These regions are called "reaction zones." At normal (atmospheric) pressures these reaction zones (i.e., preheat, primary, and secondary) are small compared to the overall flame dimensions (Fifer 1984). A low pressure environment causes the entire flame to become more diffuse, expanding the reaction zones and providing a larger region for study.

Although flames have been studied extensively since the middle of the 19th century (Gaydon 1974), there are experimental difficulties which have yet to be entirely overcome. Chief among these are the determination of temperature and the quantification of species within the flame. Ideally, any method of probing a flame should be quantitative and nonintrusive. Infrared spectroscopy is an excellent tool for such studies, but has the disadvantage that it is a line-of-sight technique, and therefore its value as a diagnostic tool is degraded when the beam must traverse a nonhomogeneous medium.

In this study, we report results from an analysis of a low pressure stoichiometric methane/nitrous oxide flowing mixture prior to and during combustion using Fourier transform infrared (FT-IR) spectroscopy. As mentioned above, the main disadvantage to using line-of-sight absorption techniques is that the signal at the detector is determined by species along the entire beam path. In low pressure flame work, large temperature and density gradients along the beam path make it difficult to determine which features in the spectrum are from species within the flame zone, and which are due to exhaust gases, or to species within interfacial regions, or species in the beam path outside of the low pressure chamber.

Several methods have been employed to discriminate against cold gas absorptions in line-of-sight spectra of burner flames. A shroud gas is often used to provide an entertainment of combustion species within the cylinder defined by the burner frit circumference. However, the probe beam still must traverse

regions of greatly varying density and temperature. Sapphire tipped "eyeballs" may be inserted into the chamber near the flame and used to physically exclude the beam from passing through the cold gas region, but this technique has the potential to perturb the flame. Another method of cold gas discrimination is to observe transitions from states which are only populated at elevated temperatures (Ouyang and Varghese 1991). This method still is limited by the fact that the technique is a line-of-sight method, and that the observed absorbance is still integrated along a path through all temperature and density gradients.

Recently, Best et al. (1991) have published a paper describing the history and use of tomography to determine species concentrations and temperatures within an atmospheric pressure diffusion flame, and to report the first use of tomography to analyze infrared spectra. We have applied a similar technique to the analysis of line of sight spectra of subatmospheric pressure flow mixtures prior to and during combustion. We have also used the technique to reconstruct full local spectra within the cylinder defined by our burner frit circumference.

2. BACKGROUND

Classical tomography assumes any object to be composed of a series of slices that have been stacked upon each other to form the object. The objective of classical tomography is to be able to look inside an object and see any one of those slices, with the view being unobscured by the slices in front of or behind the slice of interest. Typically, in classical tomography, only the layer of interest is in focus, while other layers are blurred or do not appear at all. As employed in radiology, classical tomography moves the source (usually emitting x-rays) and the detector in such a way that only a point in the plane of interest is in focus. This is usually accomplished by making the point of interest in the plane of interest the fulcrum about which the source-detector pair is moved. A reconstruction of the slice or plane is accomplished by taking a series of projections through different points in the plane of interest (Barrett and Swindell 1981). Computed tomography differs from classical tomography in that all projections in computed tomography are taken through the plane of interest, with the projections restricted to lie in that plane. The picture of the plane of interest is then reconstructed using computer techniques.

3. EXPERIMENTAL

The low pressure burner apparatus is shown in Figure 1. The flame is supported on a water-cooled, stainless steel fritted burner (McKenna Industries, Inc). The premixed fuel/oxidizer mixture is regulated

by an MKS Instruments Model No. 147 flow controller and flows into the bottom of the burner into a small volume directly below the porous frit. The stainless steel burner frit (6-cm diameter) is surrounded by a porous bronze annulus, through which a shroud gas may be flowed. The burner is mounted on a motorized stage, which provides horizontal translation. This stage is, in turn, mounted on a rotatable vertical positioning device, thus providing the capability of positioning the burner at any point within a Cartesian coordinate system defined by the ranges of the positioning devices. This whole assembly sits inside an evacuable chamber which has been equipped with LiF windows. A combined fuel/oxidizer flow rate of 2 L/min is typical to support a 30-torr flame.

Figure 2 shows the experimental apparatus used to probe the flame. The output beam from a Mattson Instruments Galaxy Series FT-IR spectrometer is passed through the center of the low pressure chamber. The output beam of the FT-IR spectrometer is brought to a focus at the center of the burner chamber (unapertured beam waist of ~1 cm). Detection of the interferogram output of the FT-IR spectrometer is by a liquid nitrogen-cooled HgCdTE detector. All spectra are obtained using 200 scans at 4-cm^{-1} resolution. Maximum apertured probe beam diameter is 4.7 mm. The output of the HgCdTe detector is transformed using triangular apodization. No zero filling is employed prior to the transformation of the interferogram. Also, no adjustment was made to account for any nonlinearity of the detector when exposed to the high thermal signal from the burner flame, since the thermal emission of the flame differs as different vertical positions in the flame are imaged. Normally, this introduces a DC offset to the signal reported by the detector. However, since only the probe beam is modulated, signal detection is not noticeably affected.

Figure 3 shows an example of the probe beam path for the experiments reported here. Assuming that the beam passes through a nonabsorbing medium outside of the burner chamber, there are three distinct regions of temperature and density within the burner chamber (exhaust, shroud, burner). Proceeding from the edge of the chamber to the burner center, the gas temperature increases and the gas density decreases. This means that a volume of exhaust gas outside the burner region (lower temperature, higher density) will absorb more strongly than the same volume of exhaust gas in the burner region (higher temperature, lower density). We believe the presence of exhaust gases accounts for the lower than expected temperatures often calculated from line-of-sight spectra (McNesby and Fifer 1991).

4. METHOD OF DATA REDUCTION

In the tomographic analysis employed here, the column of premixed gas and flame (if present) above the burner frit is assumed to have axial symmetry. Referring to Figure 4, let f(p) be the line-of-sight absorbance along a path normal to a radius vector r, where p is the distance of the normal to the path to the burner axis. The line-of-sight absorbance f(p) at a particular frequency is given by

$$f(p) = 2\int_p^1 g(r)rdr/(r^2 - p^2) , \qquad (1)$$

where g(r) is the radial dependance of the absorbance at a particular frequency. Figure 5 shows f(p) as a function of p for a constant g(r) and for a triangular g(r). Equation 1 is one half of an Abel inversion pair (Cormack 1963), the other equation being

$$g(r) = -d/dr\,\{\pi/r\int_r^1 f(p)dp/[p(p^2 - r^2)]\} . \qquad (2)$$

Figure 6 shows the result of inverting the synthetic data for the constant g(r) shown in Figure 5, with and without line-of-sight data through regions where the absorbance is zero, for 23 and 20 evenly spaced data points, respectively. The g(r) retrieved by the inversion agrees well with that input into the original calculation. The "ringing" observed in the region of transition between constant and zero absorbance decreases as the number of evenly spaced data points increases. The inversion program was kindly provided by Prof. Philip Varghese of the University of Texas (Deutsch and Beniaminy 1983).

5. RESULTS AND DISCUSSION FROM TOMOGRAPHIC ANALYSIS OF EXPERIMENTAL DATA

The tomographic technique just described is first applied here to a noncombusting stoichiometric CH_4/N_2O mixture, with an Argon shroud, flowing at 4.6 torr. Flow rates for the methane-nitrous oxide mixture were 0.35 and 1.3 L/min, respectively. Ar flow was 5.0 L/min. Because the technique should discriminate against all absorbances except those which change as beam position through the burner

changes, single-beam spectra are used in the analysis. Figure 7 shows a three-dimensional representation of line-of-sight single-beam spectra through the flowing $Ar/CH_4/N_2O$ mixture. These spectra represent the convolution of the source output and the detector response curves superimposed upon the absorptions due to gases in the beam path. The probe beam is centered at the lowest unobscured position relative to the burner surface (beam center 2.3 mm above burner surface). The absorption caused by the asymmetric stretch of CO_2 (in the beam path outside of the chamber) dominates the spectrum. Features due to the C-H stretch in methane (3,020 cm^{-1}) and the asymmetric stretch in N_2O (2,223 cm^{-1}) are much less discernable. In addition, there is no appreciable diminishment in absorption due to CH_4 or N_2O for line-of-sight spectra as the edge of the burner frit (at 30 mm off-axis distance) is approached by the probe beam. Figure 8 shows the spectrum for r = 0 (i.e., at the burner center) reconstructed using Abel inversion from the data in Figure 7. For this reconstruction, the absorbance due to the asymmetric stretch of CO_2 has been almost completely removed. An absorption is shown as a negative deviation since gases present in the beam path remove intensity from the beam. The increase in noise relative to the original spectra is caused by the inversion process. Usually, some form of data smoothing (Best et al. 1991) (and accompanied decrease in spectral resolution) is performed prior to inversion of the data to minimize the noise in the transformed spectra. No smoothing of the data was performed for the spectra reported here.

Figure 9 shows a three-dimensional reconstruction of the radial dependence of the infrared spectrum of the flowing gas mixture obtained from the spectra presented in Figure 7. At the right (low frequency) side of this figure the N_2O absorption (at 2,223 cm^{-1}) is seen to diminish (become less positive) as the edge of the burner frit is approached. Similar behavior is seen at 3,020 cm^{-1} for the C-H stretch of CH_4. The unusual behavior of the absorption due to the asymmetric stretch of CO_2 is believed to be due to atmospheric fluctuations in CO_2 during the course of a given experiment, which is accentuated because the beam travels approximately 1 meter through open air between the spectrometer and the low pressure chamber. Figure 10 shows reconstructed spectra of the species present at the burner center as a function of height above the burner surface. These spectra were reconstructed from the spectra shown in Figure 7. Intensities have been normalized to 0 at 2,000 cm^{-1} to aid in comparing the spectra to each other. In general, it appears that the concentrations of methane and nitrous oxide remain nearly constant at the burner center up to 23 mm above the burner surface.

Figure 11 shows a three-dimensional representation of line-of-sight absorbance spectra taken through a stoichiometric methane/nitrous oxide flame at 40-torr total pressure. No shroud gas is used. The 4.7-mm diameter probe beam is centered 6 mm above the burner surface. Spectra are collected at 4-cm^{-1}

resolution. The spectral region shown is that corresponding to the asymmetric stretch region of CO_2 and N_2O. In this figure, the CO_2 absorbance is seen to obliterate all other features. Figure 12 shows the data from Figure 11 after inversion. The CO_2 absorbance has now almost completely disappeared and, instead, an absorbance due to N_2O (2,223 cm^{-1}) is the most prominent feature in the spectra. The broad profile of the N_2O absorption is believed to be caused by the temperature gradient which occurs along the distance defined by the probe beam diameter (4.7 mm). This reconstruction indicates that the CO_2 absorbance in Figure 11 is due to gas outside the cylindrical region proscribed by the burner frit circumference. No absorbance due to CH_4 at 3,020 cm^{-1} was observed in either the raw or transformed spectra. The gradual sloping of the absorbances as off-axis distance (p) increases in the inverted spectra in Figure 12, may in part be caused by the limited number (8) of data points.

6. CONCLUSIONS

We believe that tomographic analysis of line-of-sight spectra through inhomogeneous media will become a standard analytical technique. While many experimental and computational difficulties remain, the degree of sophistication already employed in radiological imaging will undoubtedly accelerate development of tomography as a spectroscopic technique. We are engaged in an ongoing research project which is applying tomographic analysis to laser spectroscopy and Fourier transform spectroscopy with the aim of being able to spatially quantify all infrared active species within the burner flame. At present, our immediate goal is to increase the number of projections obtainable with the Fourier transform spectrometer, since the quality of the reconstruction increases with the number of projections. We believe this will become a valuable tool in combustion spectroscopy. We are also developing an application of the technique to FT-IR microscopy.

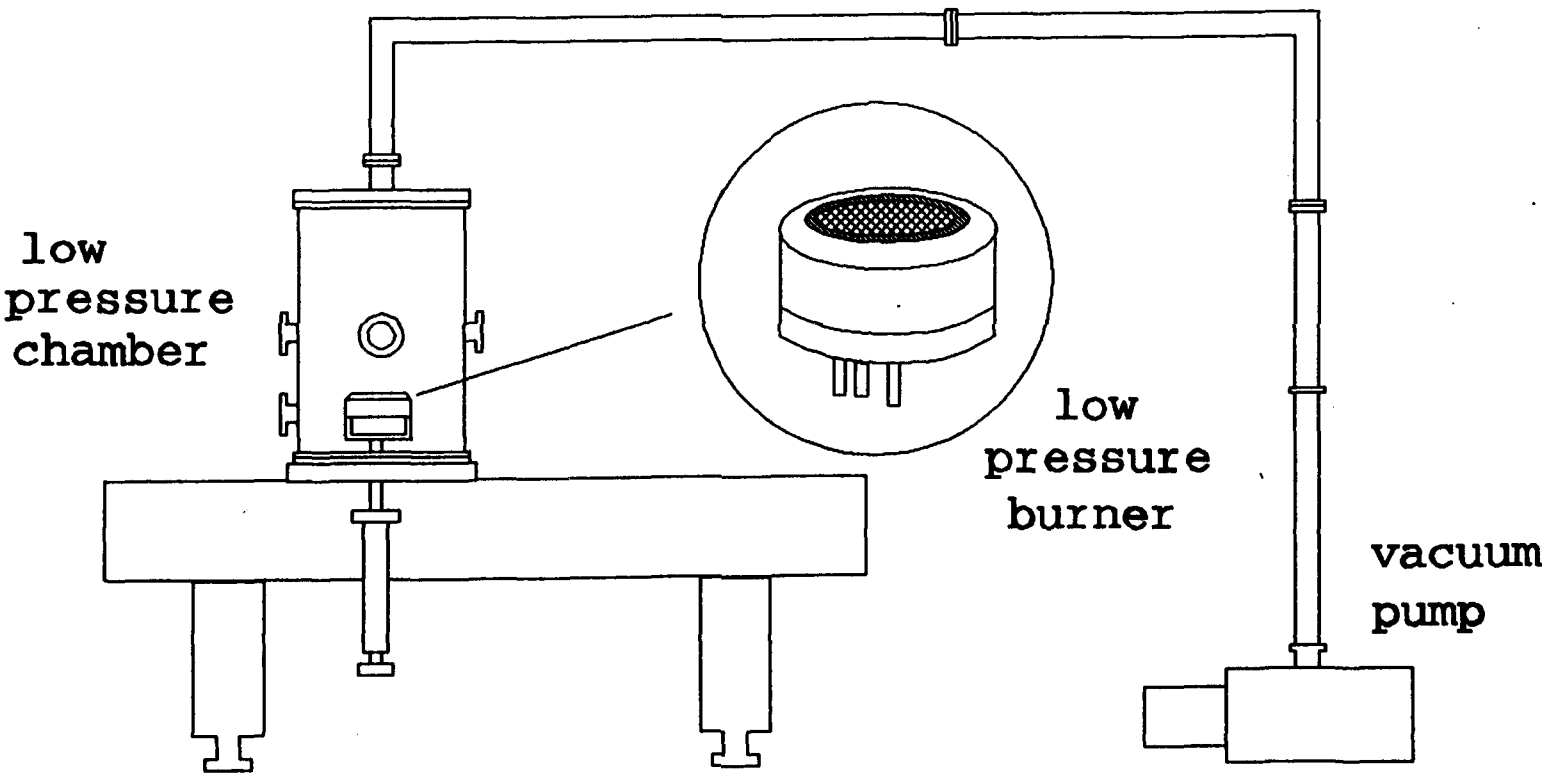

Figure 1. The Low Pressure Burner Apparatus Used in the Experiments, Showing the Burner Inside Evacuable Housing.

Legend: p=parabaloid mirror
e=ellipsoid mirror
f=flat mirror
w=LiF window
b=burner
d=detector

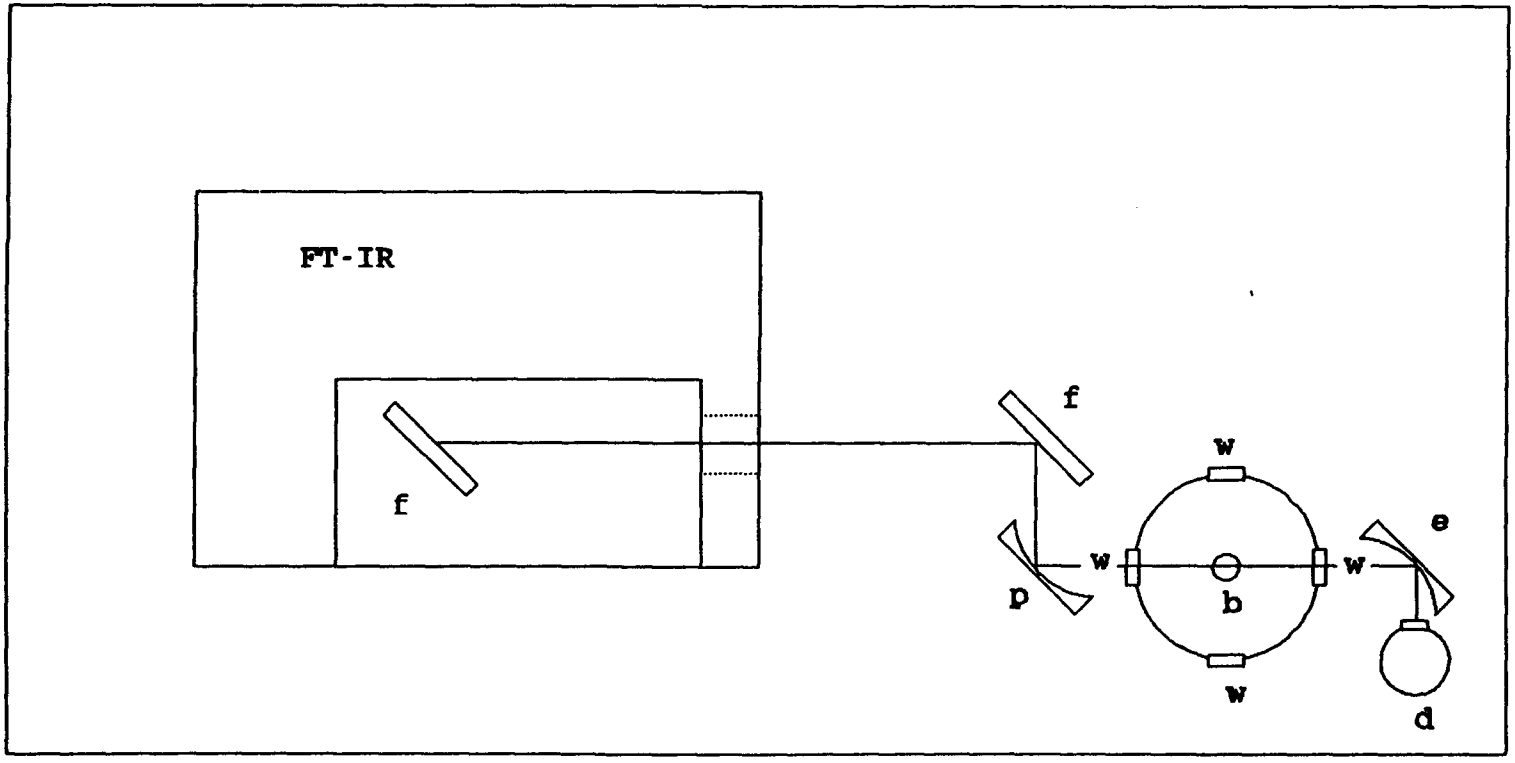

Figure 2. The Experimental Apparatus Used to Probe Low Pressure Flames.

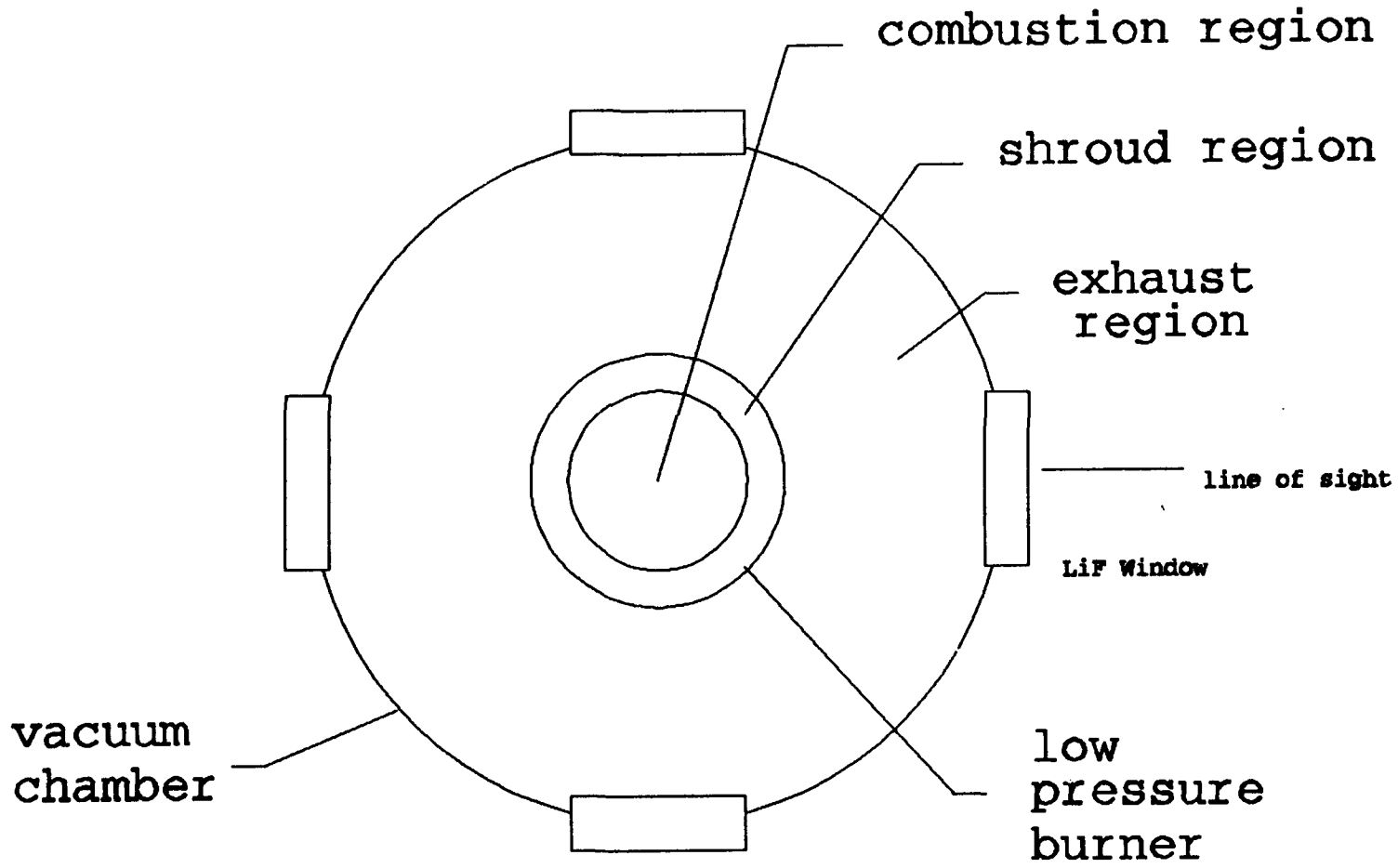

Figure 3. The Different Regions Traversed by the Probe Beam in Infrared Absorption Measurements of Low Pressure Flames.

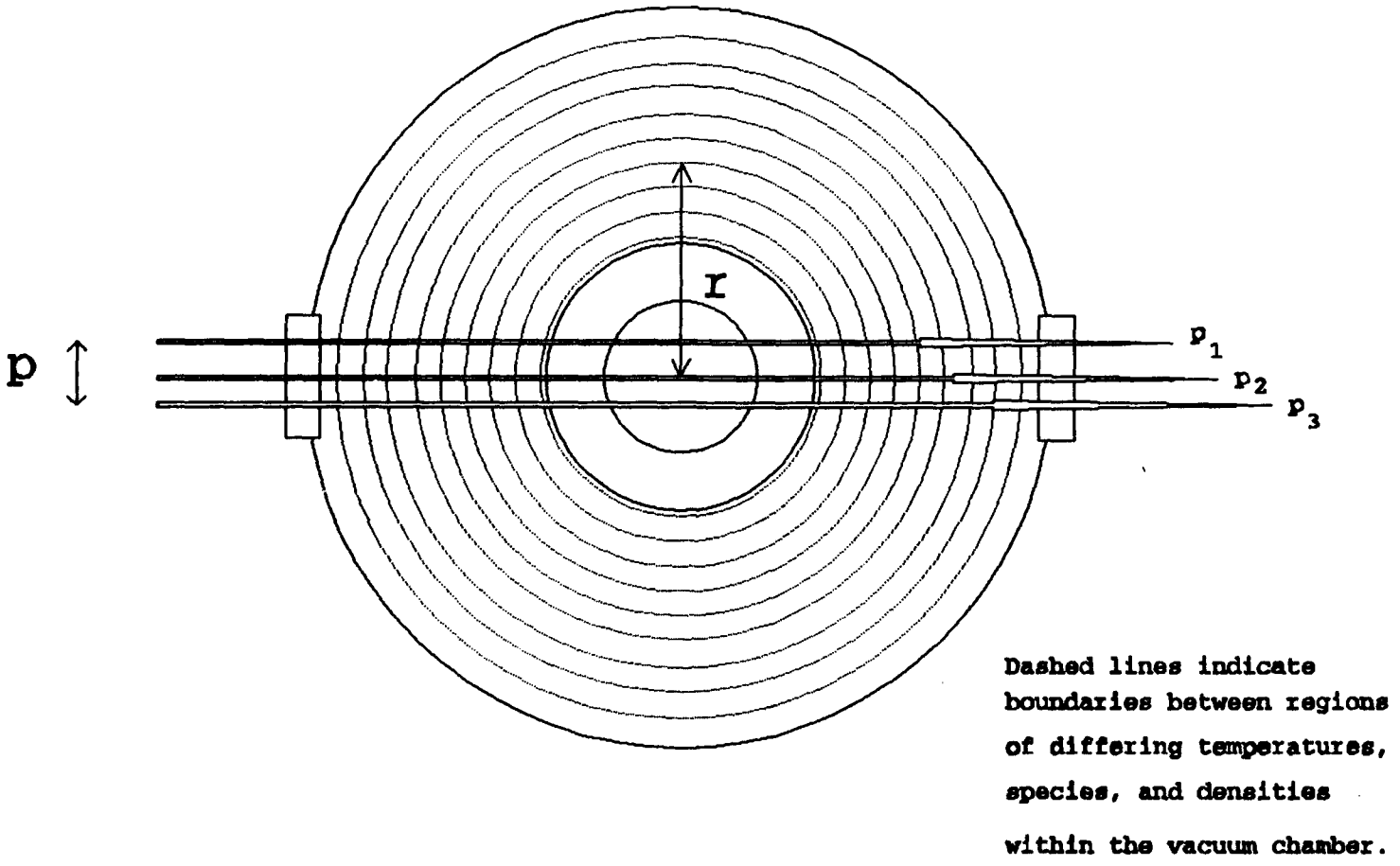

Figure 4. A Description of the Line-of-Sight Measurements Used for Tomographic Analysis of Data.

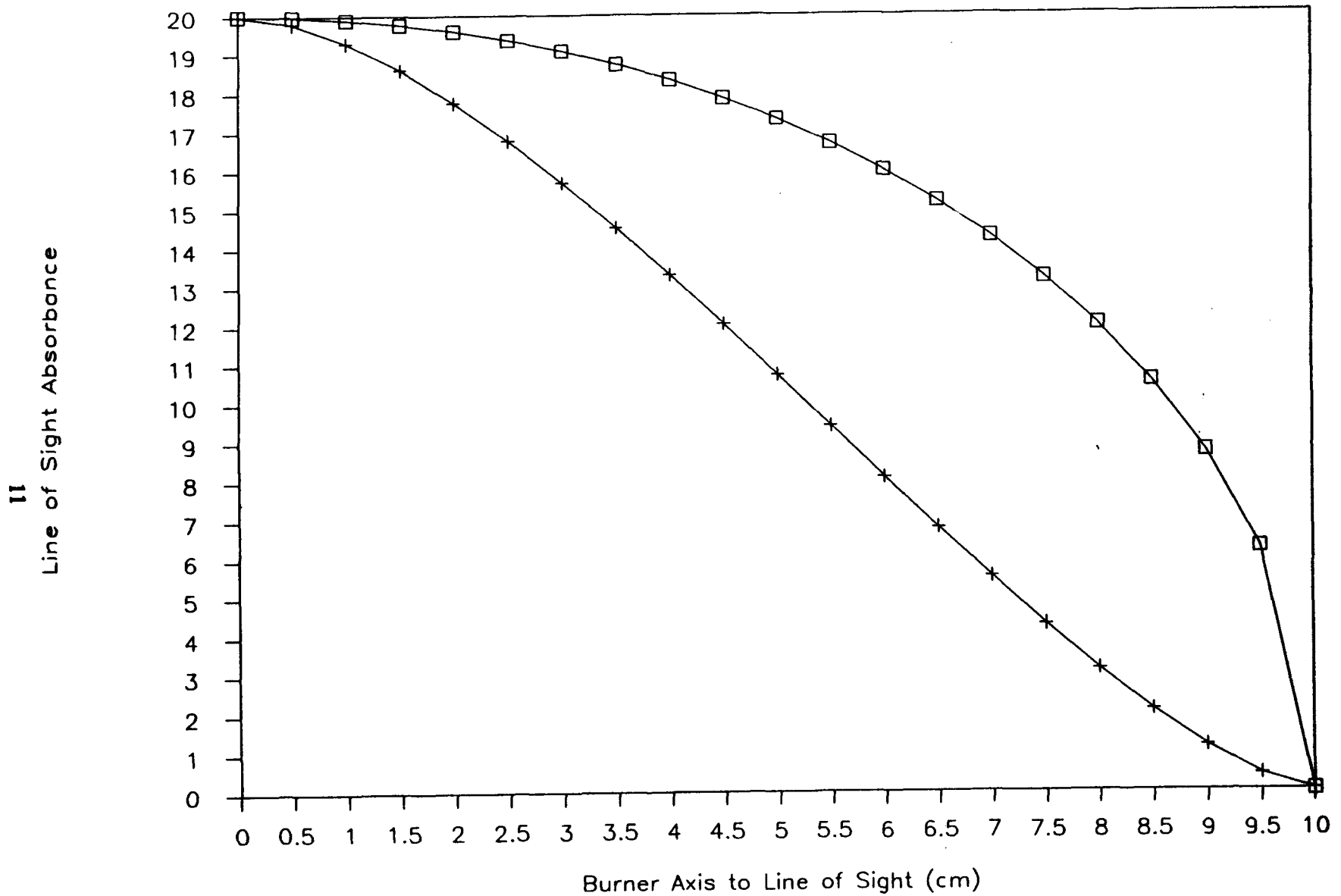

Figure 5. Synthetic Line-of-Sight Absorbances as a Function of Off-Axis Position for Constant and Varying g(r). Plusses Denote $g(r) = A_o(1 - r/D)$. Squares Denote $g(r) = A_o$. D is the Burner Diameter.

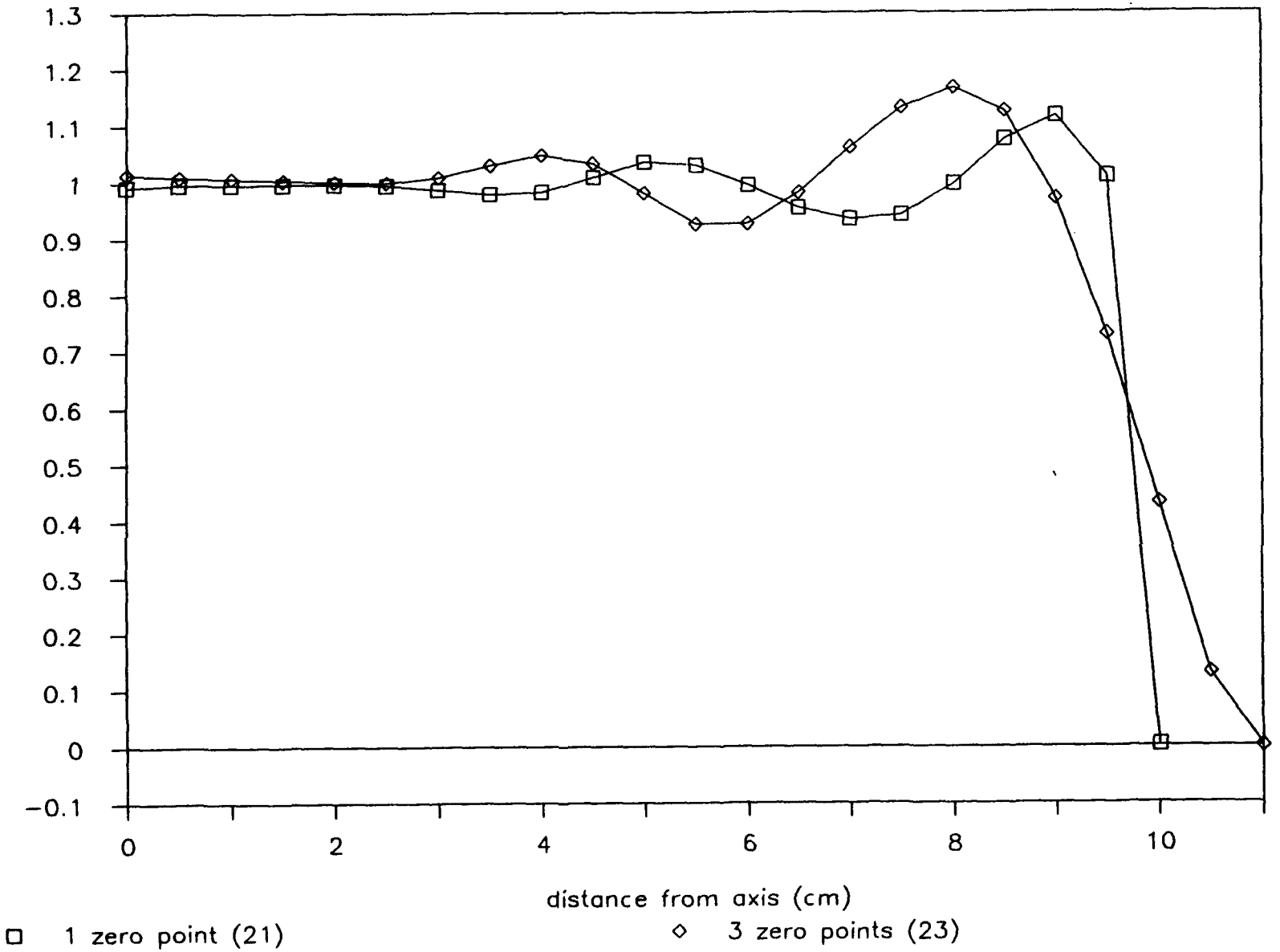

Figure 6. Inverted Synthetic Data for Constant g(r) Using 21 and 23 Data Points.

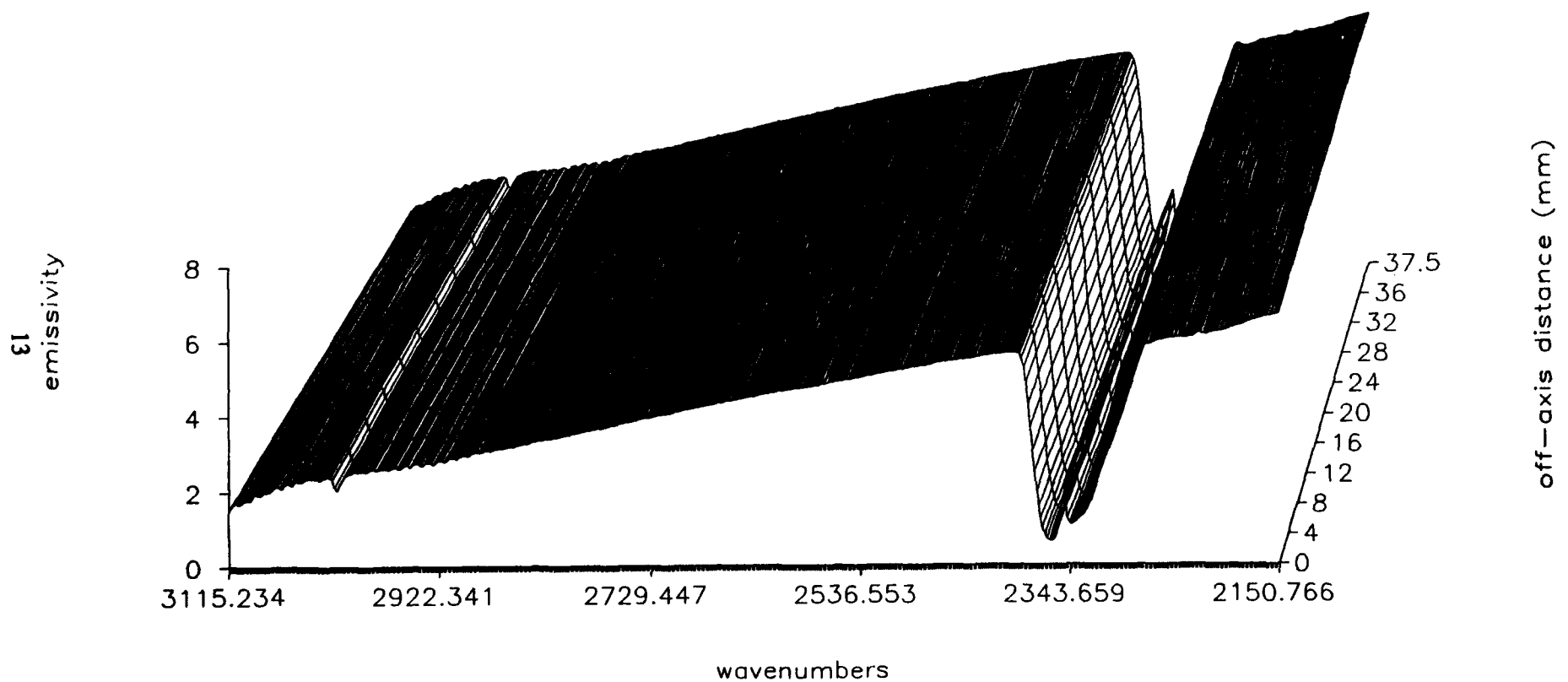

Figure 7. Line-of-Sight Beam Spectra Through a Flowing Ar/CH_4/N_2O Mixture at 4.5 torr.

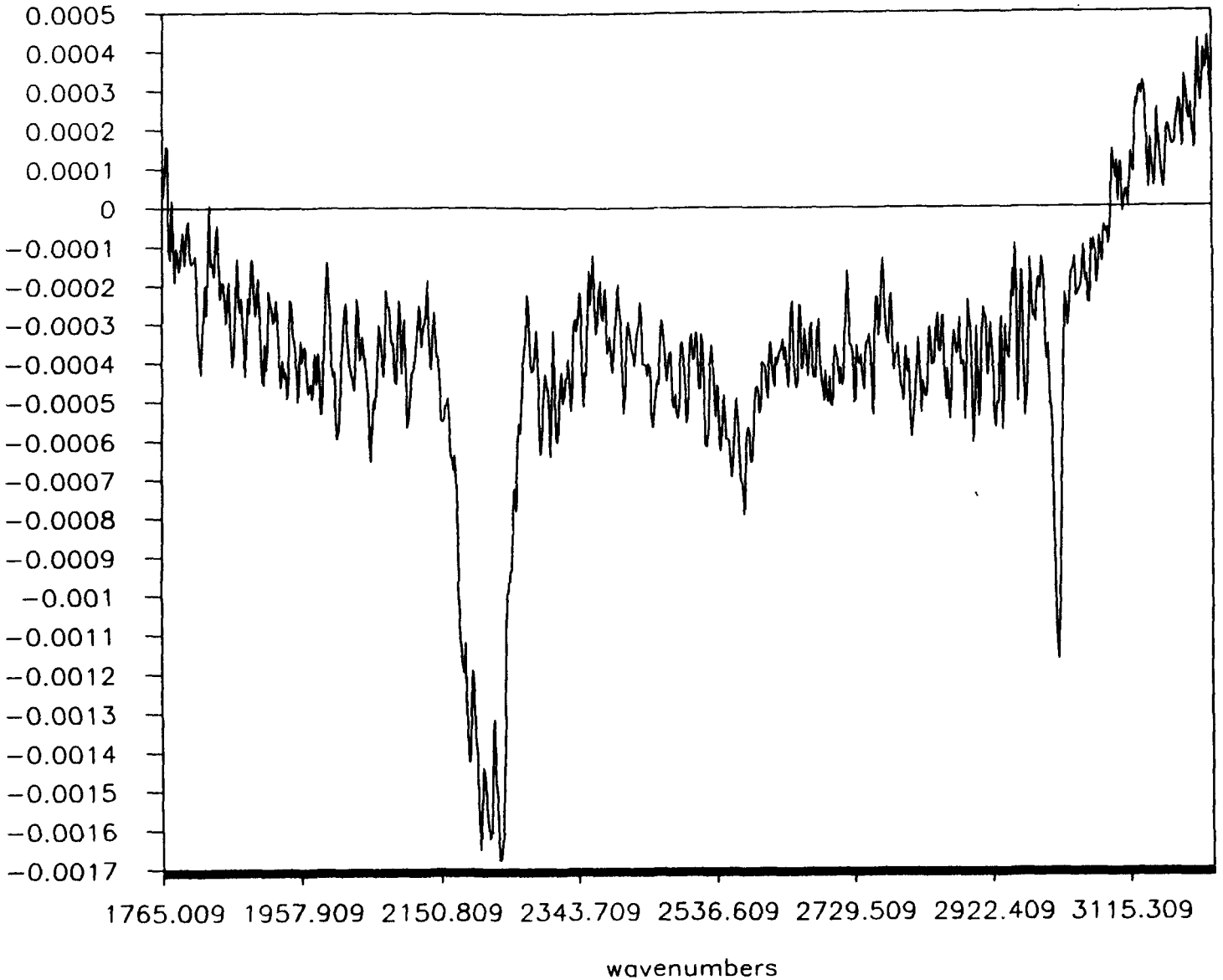

Figure 8. Infrared Spectrum at the Burner Center (r = 0) Reconstructed From the Data Shown in Figure 7.

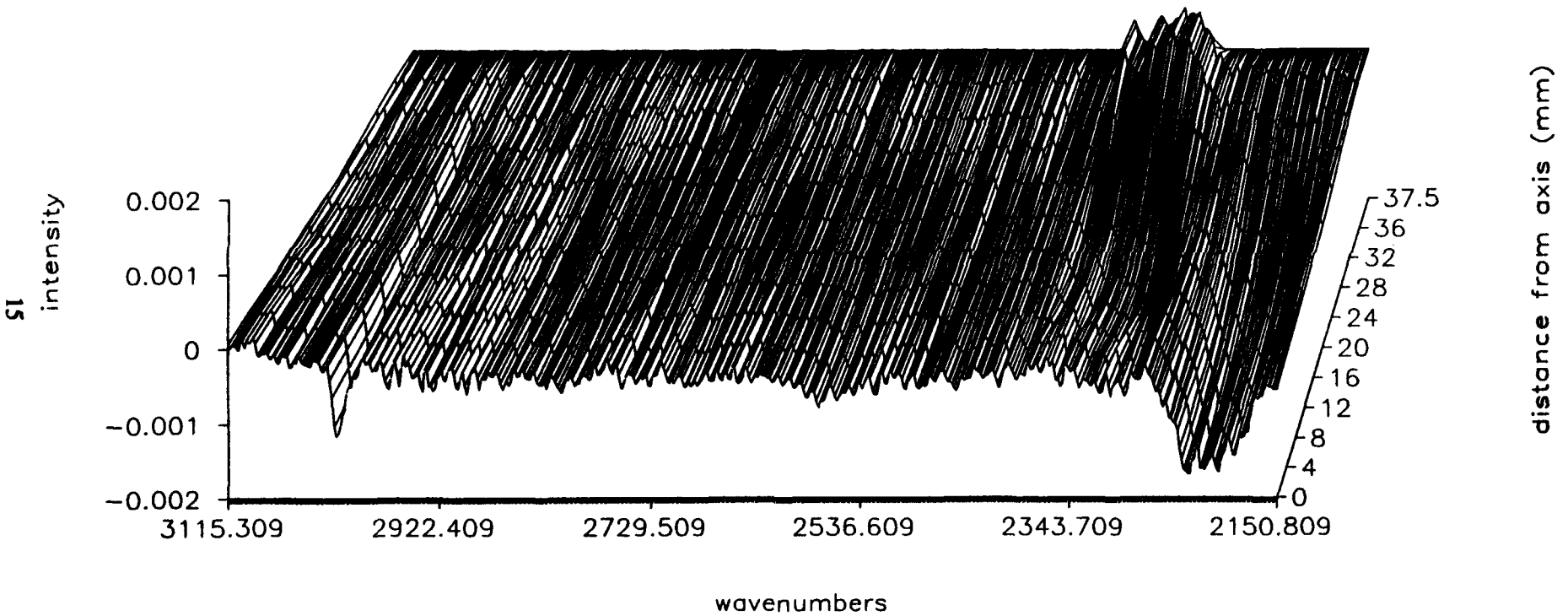

Figure 9. Radial Dependence of the Infrared Spectrum of the Flowing $Ar/CH_4/N_2O$ Mixture Reconstructed From the Data Shown in Figure 7.

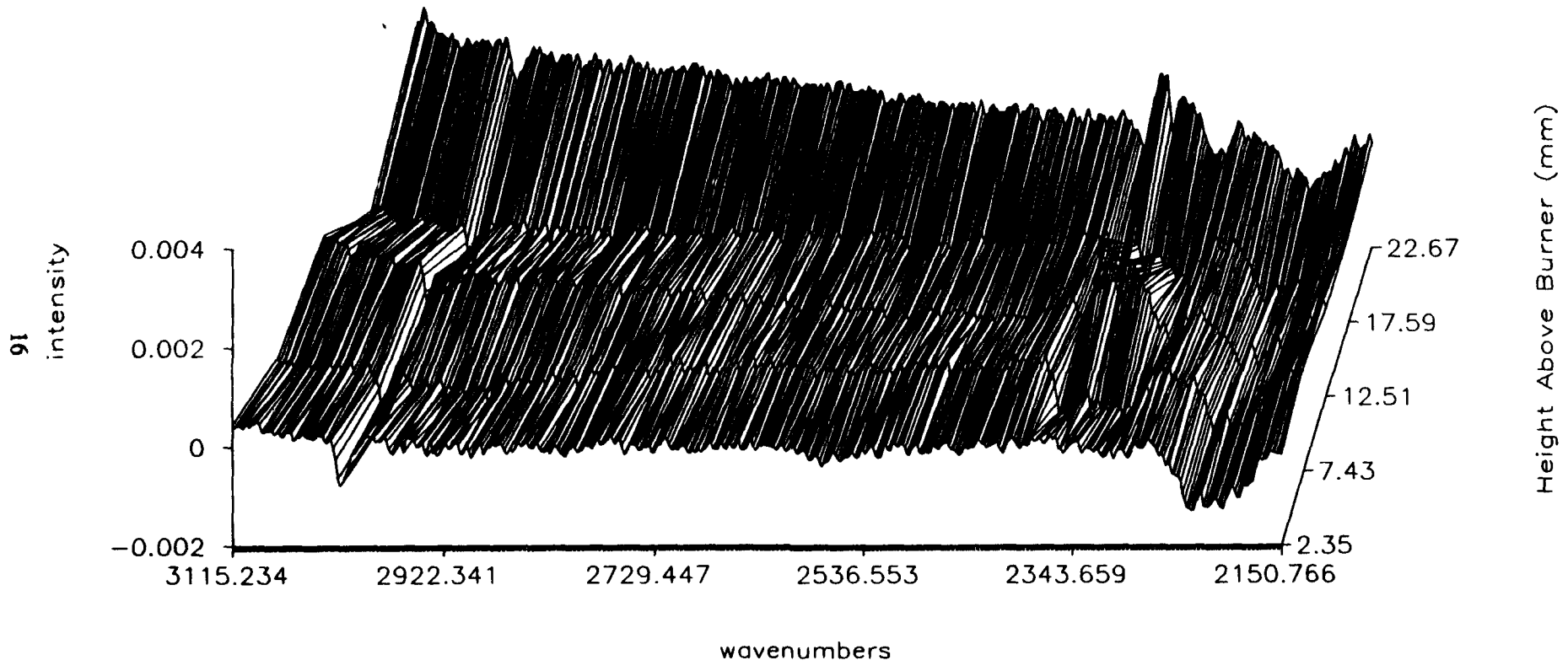

Figure 10. Infrared Spectra at the Burner Center (r = 0) for the Flowing Ar/CH_4/N_2O Mixture as a Function of Height Above the Burner Surface.

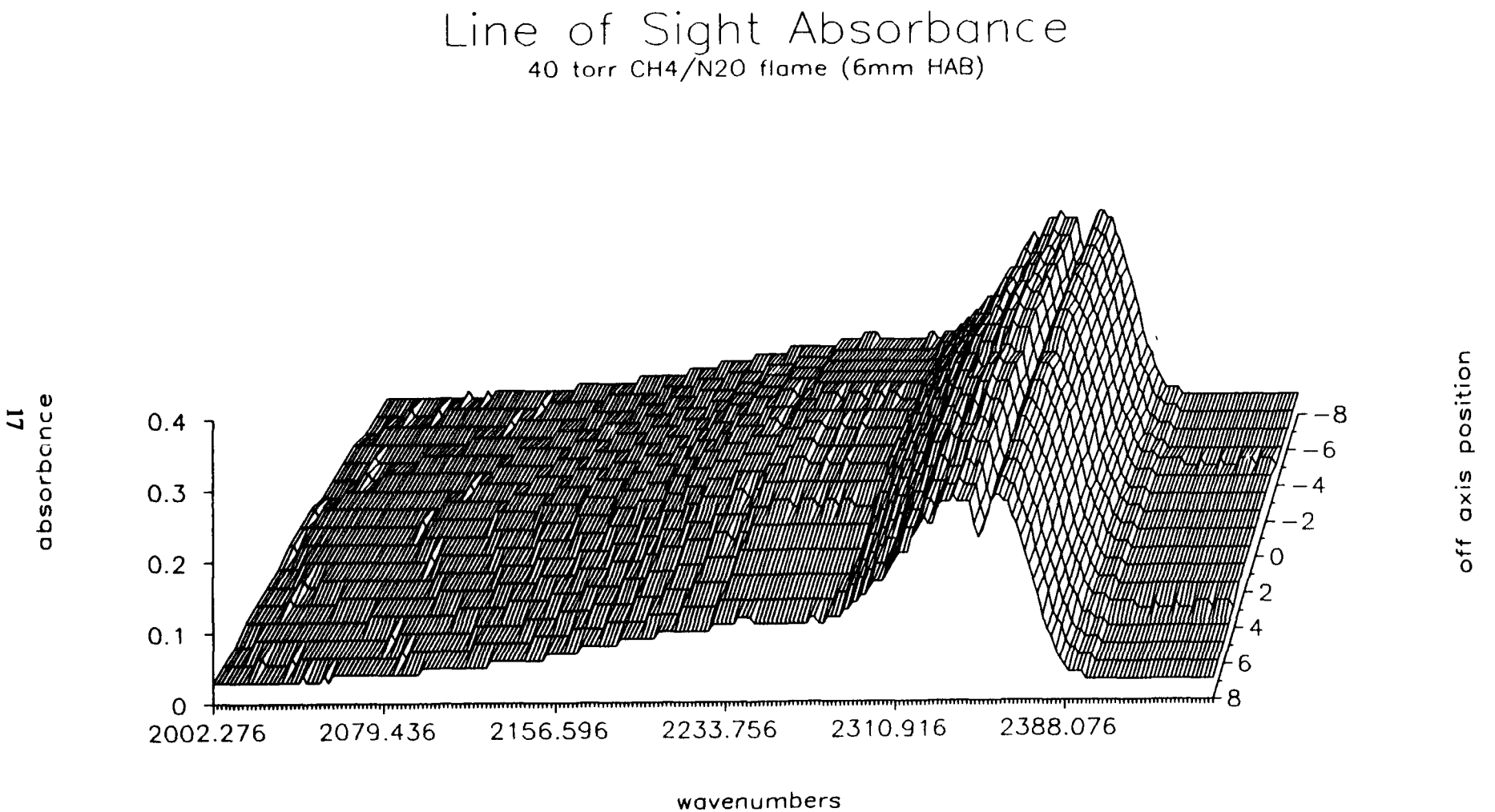

Figure 11. Line-of-Sight Absorption Spectra Through a 40-torr Stoichiometric CH_4/N_2O Flame. Data Has Been Reflected About the Burner Axis. Off-Axis Position in Units of 3 mm.

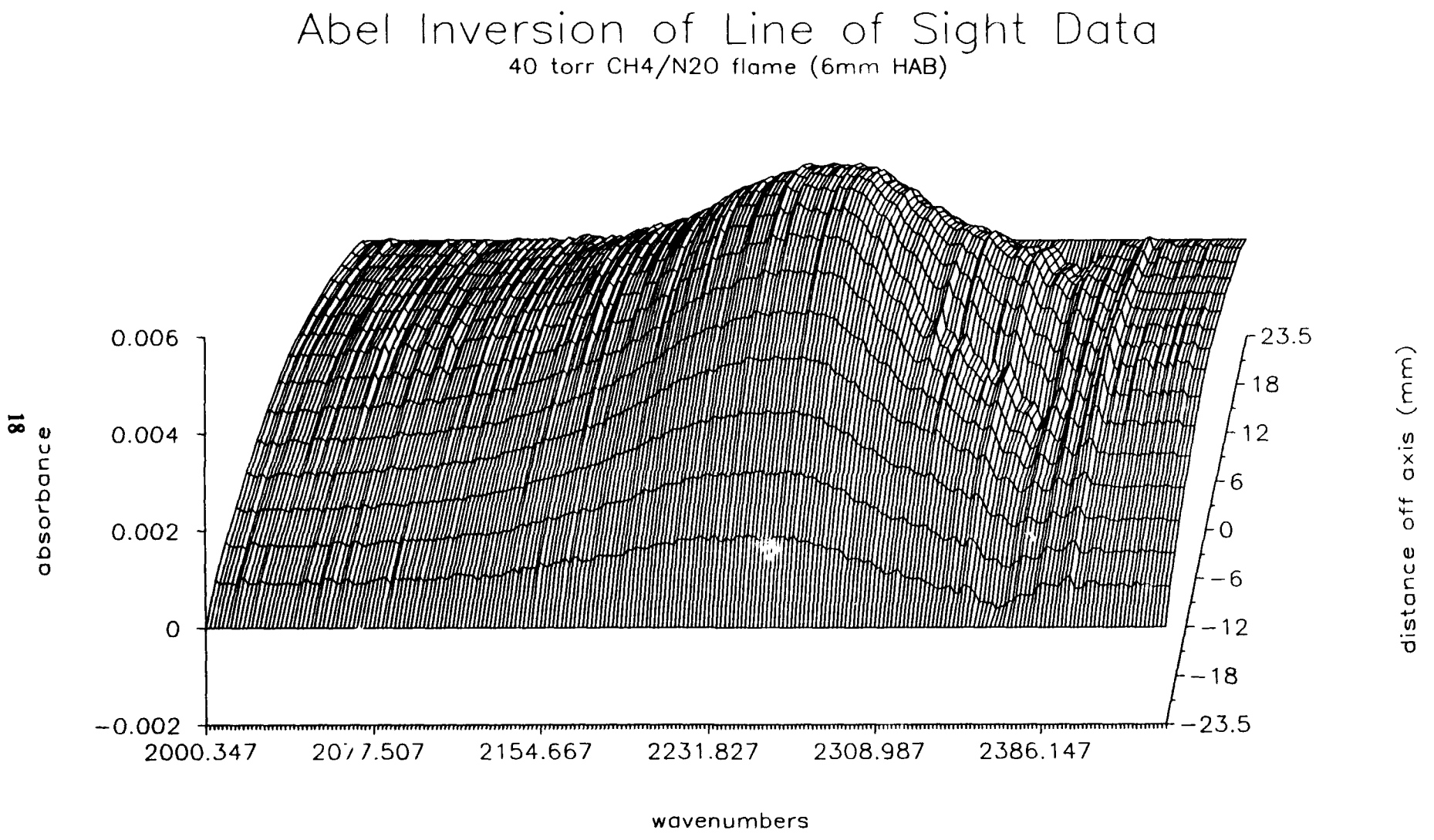

Figure 12. Inverted Data From Figure 11 Showing Almost Complete Discrimination of Absorbance Due to CO_2. Data Has Been Reflected About the Burner Axis.

7. REFERENCES

Barrett, H. H., and W. Swindell. Radiological Imaging. NY: Academic Press, 1981.

Best, P. E., P. L. Chien, R. M. Carangelo, P. R. Solomon, M. Danchak, and I. Ilovici. "Tomographic Reconstruction of FT-IR Emission and Transmission Spectra in a Sooting Laminar Diffusion Flame: Species Concentrations and Temperatures." Combustion and Flame, vol. 85, pp. 309–318, 1991.

Cormack, A. M. "Representation of a Function by Its Line Integrals, With Some Radiological Implications." Journal of Applied Physics, vol. 34, pp. 2722–2727, 1963.

Deutsch, M., and I. Beniaminy. "Inversion of Abel's Integral Equation for Experimental Data." Journal of Applied Physics, vol. 54, pp. 137–143, 1983.

Fifer, R. A. "Fundamentals of Solid Propellant Combustion." Progress in Astronautics and Aeronautics, vol. 90, K. Kuo and M. Summerfield, editors, AIAA, Washington, DC, 1984.

Gaydon, A. G. The Spectroscopy of Flames. NY: Wiley & Sons, 1974.

McNesby, K. L., and R. A. Fifer. "Rotational Temperature Estimation of CO at High Temperatures by Graphical Methods Using FT-IR Spectrometry." Applied Spectroscopy, vol. 45, pp. 61–67, 1991.

Ouyang, X., and P. L. Varghese. "Selection of Spectral Lines for Combustion Diagnostics." Applied Optics, vol. 29, pp. 4884–4890, 1991.

Schroeder, M. A. Proceeding of the Seventeenth JANNAF Combustion Meeting. CPIA Publication 329, vol. 2, Johns Hopkins University, Applied Physics Laboratory, Laurel, MD, 1980.

INTENTIONALLY LEFT BLANK.

No. of Copies	Organization
2	Administrator Defense Technical Info Center ATTN: DTIC-DDA Cameron Station Alexandria, VA 22304-6145
1	Commander U.S. Army Materiel Command ATTN: AMCAM 5001 Eisenhower Ave. Alexandria, VA 22333-0001
1	Commander U.S. Army Laboratory Command ATTN: AMSLC-DL 2800 Powder Mill Rd. Adelphi, MD 20783-1145
2	Commander U.S. Army Armament Research, Development, and Engineering Center ATTN: SMCAR-IMI-I Picatinny Arsenal, NJ 07806-5000
2	Commander U.S. Army Armament Research, Development, and Engineering Center ATTN: SMCAR-TDC Picatinny Arsenal, NJ 07806-5000
1	Director Benet Weapons Laboratory U.S. Army Armament Research, Development, and Engineering Center ATTN: SMCAR-CCB-TL Watervliet, NY 12189-4050
(Unclass. only)1	Commander U.S. Army Armament, Munitions, and Chemical Command ATTN: AMSMC-IMF-L Rock Island, IL 61299-5000
1	Director U.S. Army Aviation Research and Technology Activity ATTN: SAVRT-R (Library) M/S 219-3 Ames Research Center Moffett Field, CA 94035-1000
1	Commander U.S. Army Missile Command ATTN: AMSMI-RD-CS-R (DOC) Redstone Arsenal, AL 35898-5010

No. of Copies	Organization
1	Commander U.S. Army Tank-Automotive Command ATTN: ASQNC-TAC-DIT (Technical Information Center) Warren, MI 48397-5000
1	Director U.S. Army TRADOC Analysis Command ATTN: ATRC-WSR White Sands Missile Range, NM 88002-5502
1	Commandant U.S. Army Field Artillery School ATTN: ATSF-CSI Ft. Sill, OK 73503-5000
2	Commandant U.S. Army Infantry School ATTN: ATZB-SC, System Safety Fort Benning, GA 31903-5000
(Class. only)1	Commandant U.S. Army Infantry School ATTN: ATSH-CD (Security Mgr.) Fort Benning, GA 31905-5660
(Unclass. only)1	Commandant U.S. Army Infantry School ATTN: ATSH-CD-CSO-OR Fort Benning, GA 31905-5660
1	WL/MNME Eglin AFB, FL 32542-5000
	Aberdeen Proving Ground
2	Dir, USAMSAA ATTN: AMXSY-D AMXSY-MP, H. Cohen
1	Cdr, USATECOM ATTN: AMSTE-TC
3	Cdr, CRDEC, AMCCOM ATTN: SMCCR-RSP-A SMCCR-MU SMCCR-MSI
1	Dir, VLAMO ATTN: AMSLC-VL-D
10	Dir, USABRL ATTN: SLCBR-DD-T

No. of Copies	Organization
1	HQDA (SARD-TC, C.H. Church) WASH DC 20310-0103
4	Commander US Army Research Office ATTN: R. Ghirardelli D. Mann R. Singleton R. Shaw P.O. Box 12211 Research Triangle Park, NC 27709-2211
2	Commander US Army Armament Research, Development, and Engineering Center ATTN: SMCAR-AEE-B, D.S. Downs SMCAR-AEE, J.A. Lannon Picatinny Arsenal, NJ 07806-5000
1	Commander US Army Armament Research, Development, and Engineering Center ATTN: SMCAR-AEE-BR, L. Harris Picatinny Arsenal, NJ 07806-5000
2	Commander US Army Missile Command ATTN: AMSMI-RD-PR-E, A.R. Maykut AMSMI-RD-PR-P, R. Betts Redstone Arsenal, AL 35898-5249
1	Office of Naval Research Department of the Navy ATTN: R.S. Miller, Code 432 800 N. Quincy Street Arlington, VA 22217
1	Commander Naval Air Systems Command ATTN: J. Ramnarace, AIR-54111C Washington, DC 20360
1	Commander Naval Surface Warfare Center ATTN: J.L. East, Jr., G-23 Dahlgren, VA 22448-5000

No. of Copies	Organization
2	Commander Naval Surface Warfare Center ATTN: R. Bernecker, R-13 G.B. Wilmot, R-16 Silver Spring, MD 20903-5000
5	Commander Naval Research Laboratory ATTN: M.C. Lin J. McDonald E. Oran J. Shnur R.J. Doyle, Code 6110 Washington, DC 20375
1	Commanding Officer Naval Underwater Systems Center Weapons Dept. ATTN: R.S. Lazar/Code 36301 Newport, RI 02840
2	Commander Naval Weapons Center ATTN: T. Boggs, Code 388 T. Parr, Code 3895 China Lake, CA 93555-6001
1	Superintendent Naval Postgraduate School Dept. of Aeronautics ATTN: D.W. Netzer Monterey, CA 93940
3	AL/LSCF ATTN: R. Corley R. Geisler J. Levine Edwards AFB, CA 93523-5000
1	AFOSR ATTN: J.M. Tishkoff Bolling Air Force Base Washington, DC 20332
1	OSD/SDIO/IST ATTN: L. Caveny Pentagon Washington, DC 20301-7100

No. of Copies	Organization
1	Commandant USAFAS ATTN: ATSF-TSM-CN Fort Sill, OK 73503-5600
1	F.J. Seiler ATTN: S.A. Shackleford USAF Academy, CO 80840-6528
1	University of Dayton Research Institute ATTN: D. Campbell AL/PAP Edwards AFB, CA 93523
1	NASA Langley Research Center Langley Station ATTN: G.B. Northam/MS 168 Hampton, VA 23365
4	National Bureau of Standards ATTN: J. Hastie M. Jacox T. Kashiwagi H. Semerjian US Department of Commerce Washington, DC 20234
1	Aerojet Solid Propulsion Co. ATTN: P. Micheli Sacramento, GA 95813
1	Applied Combustion Technology, Inc. ATTN: A.M. Varney P.O. Box 607885 Orlando, FL 32860
2	Applied Mechanics Reviews The American Society of Mechanical Engineers ATTN: R.E. White A.B. Wenzel 345 E. 47th Street New York, NY 10017
1	Atlantic Research Corp. ATTN: R.H.W. Waesche 7511 Wellington Road Gainesville, VA 22065

No. of Copies	Organization
1	AVCO Everett Research Laboratory Division ATTN: D. Stickler 2385 Revere Beach Parkway Everett, MA 02149
1	Battelle ATTN: TACTEC Library, J. Huggins 505 King Avenue Columbus, OH 43201-2693
1	Cohen Professional Services ATTN: N.S. Cohen 141 Channing Street Redlands, CA 92373
1	Exxon Research & Eng. Co. ATTN: A. Dean Route 22E Annandale, NJ 08801
1	General Applied Science Laboratories, Inc. 77 Raynor Avenue Ronkonkama, NY 11779-6649
1	General Electric Ordnance Systems ATTN: J. Mandzy 100 Plastics Avenue Pittsfield, MA 01203
1	General Motors Rsch Labs Physical Chemistry Department ATTN: T. Sloane Warren, MI 48090-9055
2	Hercules, Inc. Allegheny Ballistics Lab. ATTN: W.B. Walkup E.A. Yount P.O. Box 210 Rocket Center, WV 26726
1	Alliant Techsystems, Inc. Marine Systems Group ATTN: D.E. Broden/ MS MN50-2000 600 2nd Street NE Hopkins, MN 55343

No. of Copies | Organization

1 Alliant Techsystems, Inc.
ATTN: R.E. Tompkins
MN38-3300
5700 Smetana Drive
Minnetonka, MN 55343

1 IBM Corporation
ATTN: A.C. Tam
Research Division
5600 Cottle Road
San Jose, CA 95193

1 IIT Research Institute
ATTN: R.F. Remaly
10 West 35th Street
Chicago, IL 60616

2 Director
Lawrence Livermore
National Laboratory
ATTN: C. Westbrook
M. Costantino
P.O. Box 808
Livermore, CA 94550

1 Lockheed Missiles & Space Co.
ATTN: George Lo
3251 Hanover Street
Dept. 52-35/B204/2
Palo Alto, CA 94304

1 Director
Los Alamos National Lab
ATTN: B. Nichols, T7, MS-B284
P.O. Box 1663
Los Alamos, NM 87545

1 National Science Foundation
ATTN: A.B. Harvey
Washington, DC 20550

1 Olin Ordnance
ATTN: V. McDonald, Library
P.O. Box 222
St. Marks, FL 32355-0222

1 Paul Gough Associates, Inc.
ATTN: P.S. Gough
1048 South Street
Portsmouth, NH 03801-5423

No. of Copies | Organization

2 Princeton Combustion
Research Laboratories, Inc.
ATTN: M. Summerfield
N.A. Messina
475 US Highway One
Monmouth Junction, NJ 08852

1 Hughes Aircraft Company
ATTN: T.E. Ward
8433 Fallbrook Avenue
Canoga Park, CA 91303

1 Rockwell International Corp.
Rocketdyne Division
ATTN: J.E. Flanagan/HB02
6633 Canoga Avenue
Canoga Park, CA 91304

4 Director
Sandia National Laboratories
Division 8354
ATTN: R. Cattolica
S. Johnston
P. Mattern
D. Stephenson
Livermore, CA 94550

1 Science Applications, Inc.
ATTN: R.B. Edelman
23146 Cumorah Crest
Woodland Hills, CA 91364

3 SRI International
ATTN: G. Smith
D. Crosley
D. Golden
333 Ravenswood Avenue
Menlo Park, CA 94025

1 Stevens Institute of Tech.
Davidson Laboratory
ATTN: R. McAlevy, III
Hoboken, NJ 07030

1 Sverdrup Technology, Inc.
LERC Group
ATTN: R.J. Locke, MS SVR-2
2001 Aerospace Parkway
Brook Park, OH 44142

No. of Copies — Organization

1 Sverdrup Technology, Inc.
ATTN: J. Deur
2001 Aerospace Parkway
Brook Park, OH 44142

1 Thiokol Corporation
Elkton Division
ATTN: S.F. Palopoli
P.O. Box 241
Elkton, MD 21921

3 Thiokol Corporation
Wasatch Division
ATTN: S.J. Bennett
P.O. Box 524
Brigham City, UT 84302

1 United Technologies Research Center
ATTN: A.C. Eckbreth
East Hartford, CT 06108

3 United Technologies Corp.
Chemical Systems Division
ATTN: R.S. Brown
T.D. Myers (2 copies)
P.O. Box 49028
San Jose, CA 95161-9028

1 Universal Propulsion Company
ATTN: H.J. McSpadden
Black Canyon Stage 1
Box 1140
Phoenix, AZ 85029

1 Veritay Technology, Inc.
ATTN: E.B. Fisher
4845 Millersport Highway
P.O. Box 305
East Amherst, NY 14051-0305

1 Brigham Young University
Dept. of Chemical Engineering
ATTN: M.W. Beckstead
Provo, UT 84058

1 California Institute of Tech.
Jet Propulsion Laboratory
ATTN: L. Strand/MS 512/102
4800 Oak Grove Drive
Pasadena, CA 91109

No. of Copies — Organization

1 California Institute of Technology
ATTN: F.E.C. Culick/
MC 301-46
204 Karman Lab.
Pasadena, CA 91125

1 University of California
Los Alamos Scientific Lab.
P.O. Box 1663, Mail Stop B216
Los Alamos, NM 87545

1 University of California, Berkeley
Chemistry Deparment
ATTN: C. Bradley Moore
211 Lewis Hall
Berkeley, CA 94720

1 University of California, San Diego
ATTN: F.A. Williams
AMES, B010
La Jolla, CA 92093

2 University of California, Santa Barbara
Quantum Institute
ATTN: K. Schofield
M. Steinberg
Santa Barbara, CA 93106

1 University of Colorado at Boulder
Engineering Center
ATTN: J. Daily
Campus Box 427
Boulder, CO 80309-0427

2 University of Southern California
Dept. of Chemistry
ATTN: S. Benson
C. Wittig
Los Angeles, CA 90007

1 Cornell University
Department of Chemistry
ATTN: T.A. Cool
Baker Laboratory
Ithaca, NY 14853

No. of Copies	Organization
1	University of Delaware ATTN: T. Brill Chemistry Department Newark, DE 19711
1	University of Florida Dept. of Chemistry ATTN: J. Winefordner Gainesville, FL 32611
3	Georgia Institute of Technology School of Aerospace Engineering ATTN: E. Price W.C. Strahle B.T. Zinn Atlanta, GA 30332
1	University of Illinois Dept. of Mech. Eng. ATTN: H. Krier 144MEB, 1206 W. Green St. Urbana, IL 61801
1	Johns Hopkins University/APL Chemical Propulsion Information Agency ATTN: T.W. Christian Johns Hopkins Road Laurel, MD 20707
1	University of Michigan Gas Dynamics Lab Aerospace Engineering Bldg. ATTN: G.M. Faeth Ann Arbor, MI 48109-2140
1	University of Minnesota Dept. of Mechanical Engineering ATTN: E. Fletcher Minneapolis, MN 55455
3	Pennsylvania State University Applied Research Laboratory ATTN: K.K. Kuo H. Palmer M. Micci University Park, PA 16802

No. of Copies	Organization
1	Pennsylvania State University Dept. of Mechanical Engineering ATTN: V. Yang University Park, PA 16802
1	Polytechnic Institute of NY Graduate Center ATTN: S. Lederman Route 110 Farmingdale, NY 11735
2	Princeton University Forrestal Campus Library ATTN: K. Brezinsky I. Glassman P.O. Box 710 Princeton, NJ 08540
1	Purdue University School of Aeronautics and Astronautics ATTN: J.R. Osborn Grissom Hall West Lafayette, IN 47906
1	Purdue University Department of Chemistry ATTN: E. Grant West Lafayette, IN 47906
2	Purdue University School of Mechanical Engineering ATTN: N.M. Laurendeau S.N.B. Murthy TSPC Chaffee Hall West Lafayette, IN 47906
1	Rensselaer Polytechnic Inst. Dept. of Chemical Engineering ATTN: A. Fontijn Troy, NY 12181
1	Stanford University Dept. of Mechanical Engineering ATTN: R. Hanson Stanford, CA 94305

No. of Copies	Organization
1	University of Texas Dept. of Chemistry ATTN: W. Gardiner Austin, TX 78712
1	University of Utah Dept. of Chemical Engineering ATTN: G. Flandro Salt Lake City, UT 84112
1	Virginia Polytechnic Institute and State University ATTN: J.A. Schetz Blacksburg, VA 24061
1	Freedman Associates ATTN: E. Freedman 2411 Diana Road Baltimore, MD 21209-1525

INTENTIONALLY LEFT BLANK.

USER EVALUATION SHEET/CHANGE OF ADDRESS

This laboratory undertakes a continuing effort to improve the quality of the reports it publishes. Your comments/answers below will aid us in our efforts.

1. Does this report satisfy a need? (Comment on purpose, related project, or other area of interest for which the report will be used.) _____

2. How, specifically, is the report being used? (Information source, design data, procedure, source of ideas, etc.) _____

3. Has the information in this report led to any quantitative savings as far as man-hours or dollars saved, operating costs avoided, or efficiencies achieved, etc? If so, please elaborate. _____

4. General Comments. What do you think should be changed to improve future reports? (Indicate changes to organization, technical content, format, etc.) _____

BRL Report Number BRL-TR-3333 Division Symbol _____

Check here if desire to be removed from distribution list. ____

Check here for address change. ____

Current address: Organization _____
Address _____

DEPARTMENT OF THE ARMY
Director
U.S. Army Ballistic Research Laboratory
ATTN: SLCBR-DD-T
Aberdeen Proving Ground, MD 21005-5066

OFFICIAL BUSINESS

BUSINESS REPLY MAIL
FIRST CLASS PERMIT No 0001, APG, MD

Postage will be paid by addressee

Director
U.S. Army Ballistic Research Laboratory
ATTN: SLCBR-DD-T
Aberdeen Proving Ground, MD 21005-5066

NO POSTAGE
NECESSARY
IF MAILED
IN THE
UNITED STATES